Journal of Polymers and the Environment (2022) 30:4538–4549
https://doi.org/10.1007/s10924-022-02490-6

ORIGINAL PAPER

Fabrication and characterization of multifunctional bio-safe films based on Carboxymethyl Chitosan and Saffron Petal Anthocyanin Reinforced with Copper Oxide Nanoparticles for sensing the meat freshness

Morteza Fathi[1] · Mohammad Samadi[2] · Sepideh Abbaszadeh[1] · Mohammad Reza Nourani[3]

Accepted: 18 May 2022 / Published online: 18 June 2022

Abstract

In the present study, first, saffron petal anthocyanin (SPA) and copper oxide nanoparticles (CuO-NPs) were extracted and synthesized, respectively. Then, multifunctional bio-based films based on carboxymethyl chitosan (CMCS), SPA, and CuO-NPs were fabricated using solvent casting method. The mechanical, thermal, physical, optical, antibacterial, toxicity, and pH sensitivity properties of the prepared films were evaluated. The obtained results demonstrated that simultaneous incorporation of CuO-NPs and SPA improved the mechanical, UV absorption, barrier properties as well as the thermal stability of the films. Moreover, the nanocomposite films exhibited a great antimicrobial activity against both Gram-positive (*Staphylococcus aureus*) and Gram-negative (*Escherichia coli*) bacteria. Fabricated nanocomposite films obviously exhibited color change from pink to green in acidic and alkaline media, respectively. The multifunctional films could effectively sense the freshness of lamb meat during storage time, and thus they can be introduced as pH-indicators for monitoring the freshness/spoilage of meat in real-time.

Keywords Multifunctional film · Carboxymethyl chitosan · Saffron petal anthocyanin · CuO nanoparticles · pH-indicator film

Introduction

Over the last few decades, intelligent and bio-based active films have received significant consideration in the food packaging industry due to their ability to extend the shelf life of foods [1–4]. These biopolymer-based films can be utilized as substitutes for non-degradable packaging such as polyethylene, polypropylene and polyethylene terephthalate, leading to reduction of environmental pollution problems [5]. Various bio-polymeric substances can be used for development of intelligent packaging such as cellulose [6], k-carrageenan [7], carboxymethyl chitosan [8]. Among these, carboxymethyl chitosan (CMCS), as a derivative of chitosan, is well-known for its remarkable properties, including low toxicity, biodegradability, good film-forming ability and water solubility [8]. Moreover, CMCS consists of hydroxyl and carboxymethyl functional groups that provide active sites for chemical modification [9]. All of these properties have made CMCS a suitable polymer to be applied in development of bio-based intelligent packaging. However, using neat CMCS film results in undesirable properties, owing to insignificant antioxidant potential and poor mechanical properties [10]. To overcome these challenges, it is necessary to incorporate active materials (anthocyanins and nanomaterials) into the formulation of CMCS-based film.

Anthocyanins are considered as one of the families of phenolic compounds extracted from different parts of plant such as fruits, vegetables, flowers, petals, etc. [11, 12]. These bioactive compounds have great antioxidant activity and a

✉ Mohammad Samadi
samadi.mohammad@yahoo.com

[1] Health Research Center, Life Style Institute, Baqiyatallah University of Medical Sciences, Tehran, Iran

[2] Exercise Physiology Research Center, Life Style Institute, Baqiyatallah University of Medical Sciences, Tehran, Iran

[3] Nanobiotechnology Research Center, Baqiyatallah University of Medical Sciences, Tehran, Iran

variety of colors such as violet, blue, red, which is dependent on the resource of anthocyanins [13, 14]. Because the color of anthocyanins is pH dependent, they can act as pH indicators [15]. Moreover, anthocyanins have been regarded as safe and alternatives to potentially harmful synthetic dyes [16]. Therefore, these properties motivate the use of anthocyanins as promising additives in development of intelligent packaging films to monitor the food quality.

Several studies have been incorporated different sources of anthocyanins, including mulberry, roselle, and saffron petals as pH indicators into the bio-based films to fabricate intelligent packaging systems [17–19]. Saffron petal is a large part of saffron flowers that mainly supplied in Khorasan, Iran (90% of total saffron in the world). The petal is mostly discarded during the plucking of saffron (Crocus Sativus) flowers' stigmas. However, various studies have been shown that the petal of saffron, as a source of natural anthocyanin exhibited excellent antioxidant and anticancer activities [20]. Hence, saffron petal anthocyanin (SPA) can be used as a cost-effective additive for fabrication of intelligent packaging systems. Some researchers have demonstrated that incorporating different anthocyanins into the polymer films decreased the mechanical performance of the films [21, 22]. For example, Alizadeh-Sani et al. (2021) fabricated the halochromic packaging by incorporating saffron petal anthocyanins into the biopolymer matrix. They reported that antioxidant, antibacterial, and light screening properties of the films improved by adding anthocyanins. But, the mechanical performance slightly decreased [18].

One of the most promising techniques to improve the mechanical properties of polymeric films is the application of nanoparticles [23–26]. Various research studies have been reported that the incorporation of nanoparticles into the films not only improved the mechanical properties of the films, but also enhanced their thermal stability and optical properties [27, 28]. Among various nanoparticles, copper oxide (CuO) represents outstanding properties, including photocatalytic, low-cost production, UV blocking, hydrophobic, electrical, and thermal stability that make it a suitable additive to improve the physico-chemical properties of the polymeric films [29]. To the best of our knowledge, there is no publication addressing the fabrication and characterization of the pH-indicator films based on CMCS-SPA-CuO. Therefore, in this study, CMCS-SPA-CuO nanocomposites were developed and their physical, mechanical, thermal, and morphological properties were investigated. Furthermore, the pH sensitivity and capability of the developed films to detect the spoilage of lamb meat were also examined.

Materials and methods

Materials

Carboxymethyl chitosan (CMCS) (molecular weight of 241.17 $g.mol^{-1}$, purity > 98%) was supplied by ZFZ Co., Iran. Copper acetate dihydrate and sodium hydroxide were provided by Sigma-Aldrich Chemical Co. (St. Louis, MO, USA). Saffron petals were collected from a farm near Torbat-heydarieh city (Khorasan province, Iran). Other materials and solvents were provided by Mojallali Co. (Tehran, Iran).

Synthesis of copper oxide nanoparticles (CuO-NPs)

A simple co-precipitation method was employed to synthesize CuO-NPs [30]. Briefly, 10 mL of copper acetate dihydrate solution (0.1 M) and 10 mL of sodium hydroxide (0.1 M) solution were separately prepared in two Erlenmeyer flasks at room temperature. The pH of the copper acetate dihydrate solution was adjusted to 8 with NaOH. The resulting suspension was washed several times by ethanol and deionized water, and then dried at 300 °C for 3 h.

Extraction of anthocyanin from saffron petals

A soaking method was applied to extract anthocyanins from saffron petals [31]. The prepared petals were dried at room temperature in dark and subsequently powdered by the grinder. In the next step, a distinct amount of dried powder of prepared saffron petals was mixed in aqueous medium (with a saffron petals/aqueous media ratio of 1: 30 (w/v)). The resulting mixture was shaken at room temperature for 24 h in a dark condition. After extraction, a filter paper (Whatman No. 1) was used to separate anthocyanin from saffron petals and then the resulting solution was centrifuged several times (5000 ×g for 20 min) for purification, followed by keeping at 4 °C in dark until further experiments.

Fabrication of CMCS, CMCS-SPA, and CMCS- SPA-CuO films

Bio-polymeric films based on CMCS, SPA, and CuO-NPs were fabricated by a simple solvent casting method [32]. Briefly, 1 g of CMCS was dissolved in 20 mL of distilled water under magnetic stirring at room temperature. In the next step, a certain amount of SPA (2 wt %) and CuO-NPs (0.5, 1, and 1.5 wt %) were separately dispersed in double-distilled water and then individually added to CMCS solution under continuous stirring. Subsequently, glycerol (20 wt %) was added to the solution, followed by mixing using an ultrasonic homogenizer (140 watts, UP400St,

Hielscher, Germany) under ice bath conditions to achieve homogeneous suspensions. The prepared suspensions were degassed, cast onto the Teflon plates, and dried in a vacuum oven at 30 °C for 48 h. Finally, the prepared films were kept into the desiccator to conserve the films from moisture changes. Neat CMCS films were fabricated without the incorporation of SPA and CuO-NPs. The CMCS films incorporated with SPA (2 wt %), CuO-NPs (0.5, 1, and 1.5 wt %), and both SPA with CuO-NPs were named as CMCS-SPA-2, CMCS-CuO-0.5, CMCS-SPA-2-CuO-0.5, CMCS-CuO-1, CMCS-SPA-2-CuO-1, CMCS-CuO-1.5, and CMCS-SPA-2-CuO-1.5, respectively.

Characterization of films

Field Emission scanning Electron Microscopy (FE-SEM)

FE-SEM (MIRA3-TESCAN-XMU, Czech Republic) at a 5.0 kV operating voltage with 15,000 X magnification was applied to evaluate the morphology of the synthesized CuO-NPs and CMCS, CMCS-SPA-2, CMCS-SPA-2-CuO-1 bio-based films.

Transmission Electron microscope (TEM) and dynamic light scattering (DLS)

The morphology and distribution size of synthesized CuO-NPs were investigated by a TEM (CM-120, Philips, Netherlands), and DLS analyzer (scatteroscope 1 qudix, Korea), respectively.

Fourier-Transform Infrared spectroscopy

The functional groups of the extracted SPA were evaluated by Fourier-Transform Infrared spectroscopy (FT-IR), model TENSOR, II, Bruker (Germany) with scan range of $4000-500\ cm^{-1}$ at a resolution of $4\ cm^{-1}$.

Ultraviolet-visible spectroscopy

Ultraviolet-visible (UV/VIS) spectrophotometer (T90 + from John Morris Co., Australia) equipped with Tungsten Halogen and Deuterium arc lamps source was used to investigate the absorption of CMCS, CMCS-SPA-2, and CMCS-SPA-2-CuO-1 films.

X-ray diffraction (XRD)

X-ray diffraction (XRD) analysis of synthesized CuO-NPs was carried out by XRD D8-Advance (Bruker Co., USA) with Cu kά radiation (λ = 1.5406 Å) at 40 kV operating voltage and 40 mA.

Color response of SPA solution to pH changes

A certain amount of SPA was dissolved in 10 mL of buffer solution (pH values were in the range of 2–12). These solutions were photographed after 30 min. Moreover, the absorption spectra of these solutions were investigated in the range of 400–900 nm by the Ultraviolet-visible (UV-Vis) spectroscopy (T90 + from John Morris Co., Australia).

Mechanical properties of the bio-based films

The mechanical properties of the films specimens were examined according to the ASTM D882 standard method using GOTECH Testing Machines (Model Al-3000, China) with 5 kN load cell and 10 mm/min crosshead speed at room temperature (25˚C). Three textural parameters, including tensile strength, young's modulus, and elongation at break of the bio-based films were determined.

Thermal stability of the bio-based films

Thermogravimetric analysis (TGA) (TG 209 F3 Tarsus, NETZSCH, Bavarian State, Germany) with a heating rate of 10 (^{o}C/min) under N_2 atmosphere was applied to evaluate the thermal stability of CMCS, CMCS-SPA-2, and CMCS-SPA-2-CuO-1 films.

Moisture content (MC), water solubility (WS), and water contact angle (WCA) of the bio-based films

The pieces of the developed films ($2.0 \times 2.0\ cm^2$) were weighted (W_i) and then heated at 105 °C until reach constant weight (W_f). MC of the films was calculated as follows [33]:

$$MC\,(\%) = \frac{W_i - W_f}{W_i} \times 100 \quad (1)$$

The dried bio-based films were heated at 105 °C for 24 h to reach a constant weight (W_i) and then immersed in 50 mL of the buffer solution (pH 7.0) for 24 h. Finally, the films were collected and dried to determine the final weight (W_f). The WS of these bio-based films was calculated using the following equation [33]:

$$WS\,(\%) = \frac{W_i - W_f}{W_i} \times 100 \quad (2)$$

The WCA of the bio-based films was determined using JIKAN CAG-20 contact angle meter (JIKAN Co., Iran). 4 µL of a distilled water droplet was deposited on the surface of the bio-based films at ambient temperature (ASTM D7334) and WCA was determined.

Antibacterial activity of the bio-based films

The antibacterial activity of the films was investigated against two strains of bacteria, including Gram-positive *S. aureus* (PTCC 1112 (ATCC 6538p)) and Gram-negative *E. coli* (ATCC 25,922), by agar disk diffusion method [34]. Briefly, an activated bacterial solution (80 µL) was spread evenly on Luria-Bertani (LB) agar disks, and then bio-based films were placed above on. Petri dishes were incubated at 37 °C for 24 h in a biochemical incubator. Finally, inhibition zones (mm) of the samples were determined.

Cell viability assay

The cell viability assay was performed by a method described by Kazemi-Pasarvi et al. [35]. Briefly, the toxicity of the fabricated films on human dermal fibroblast (HDF) cells was evaluated using 3-(4,5-dimethylthiazol-2-yl)-2,5-diphenyl-2 H-tetrazolium bromide (MTT) assay. In this regard, the sterile fabricated films were placed on 96 well plates. Cultured fibroblast cells in Dulbecco's Modified Eagle Medium (DMEM) were supplemented with 10% fetal bovine serum and 1% penicillin/streptomycin and were seeded on the surface of the prepared plates (10,000 cells/well). The cell viability was calculated after 24 h using the following equation:

$$\text{Survivalfraction} = \frac{\text{MeanODintestwells} - \text{MeanODincell} - \text{freewells}}{\text{MeanODincontrolwells} - \text{MeanODincell} - \text{freewells}} \quad (3)$$

The potential of cell adhesion of the fabricated films was investigated by 4′, 6-diamidino-2-phenylindole (DAPI) staining. HDF cells were seeded on 24 well plates, which were coated with sterilized bio-based films. The cells were fixed with 4% formaldehyde after 12 h incubation. In the next step, they were permeabilized with 0.5% Triton X-100 and stained with DAPI. A fluorescence microscope was used to observe the stained nucleus of adherent cells.

pH-sensitivity of bio-based film

Bio-based pH indicator films were immersed in the 5 buffer solutions with different pH levels (3, 5, 7, 9, and 11) at ambient temperature for 60 s. The change of color under this condition was photographed by a digital camera (Kodak M853, USA).

Color analysis

The color parameters (L* = lightness; a*= greenness/redness; and, b*= blueness/yellowness) of the bio-based films in different pH levels (3, 5, 7, 9 and 11) were determined by ImageJ software v 1.8.0 according to Seyedabadi et al. [36]. Moreover, the color difference (ΔE*) was calculated by the following Eq. [3]:

$$\Delta E^* = \sqrt{(L^*(\text{standard}) - L^*(\text{film}))^2 + (a^*(\text{standard}) - a^*(\text{film}))^2 + (b^*(\text{standard}) - b^*(\text{film}))^2} \quad (4)$$

where L* (92.60), a* (-0.32), and b* (-0.09) represented the color parameters of standard white plate.

Application of bio-based pH indicator film for monitoring the food sample spoilage

For this purpose, a disk-shaped pH indicator film with a diameter of 3 cm was attached inside the polypropylene box containing 100 gr of fresh lamb meat. Subsequently, the package was stored at 4 ˚C and 25 ˚C for five and three days, respectively. Color change of the bio-based pH indicator film was photographed using a digital camera (Kodak M853, USA) during storage time. At the same time, changing the pH values of the lamb meat was recorded by portable pH meter (COMBI 5000; STEP Systems GmbH, Germany). Moreover, total volatile basic nitrogen (TVBN) was measured according to Kuswandi and Nurfawaidi [37].

Statistical analysis

Shapiro-Wilk and Levene tests were respectively used to check the data for variance homogeneity and normal distribution. Subsequently, Tukey and ANOVA tests were applied to analyze multiple comparisons and the difference among the treatments, respectively. $P < 0.05$ was considered as the significance level.

Results and discussion

Characterization of synthesized CuO-NPs

Figure 1 (a) presents the XRD patterns of CuO-NPs. The characteristic peaks are detected at 2θ = 32.6° (110), 35.6° (002), 38.7° (111), 48.8° (-202), 53.5° (020), 58.2° (202), 61.5° (-113), 66.2° (022), and 68.1° (220), demonstrating the crystal structure of monoclinic of CuO (JCPDS 80–1268) [38]. FE-SEM and TEM analyses were used to evaluate the morphology of prepared CuO-NPs. Figure 1 (b), and (c) show the micrographs of CuO-NPs in two magnifications. Spherical shape-like with an approximate diameter of

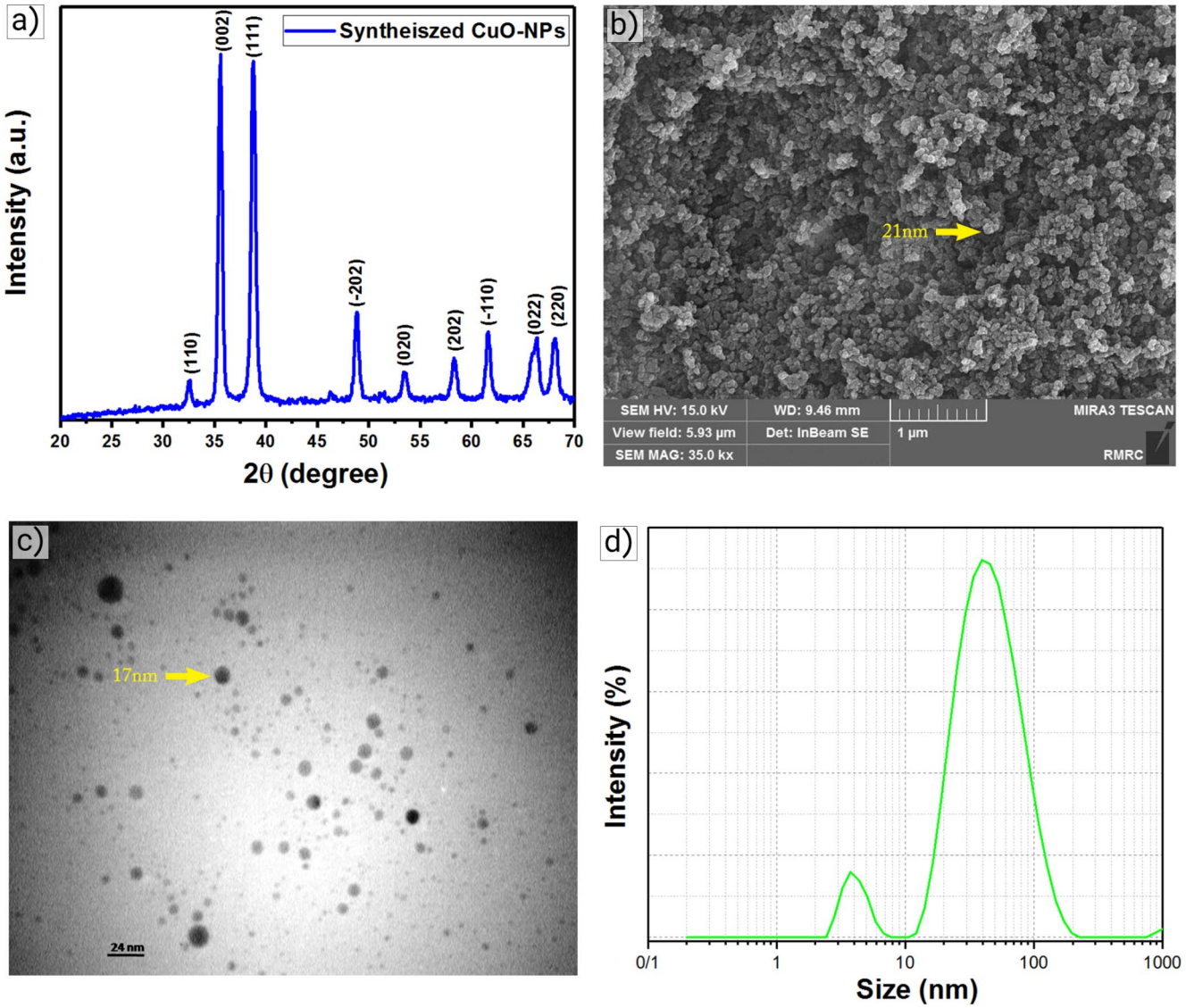

Fig. 1 Characterization of synthesized CuO-NPs: (a) XRD pattern, (b) FE-SEM micrograph, (c) TEM micrograph, and (d) DLS histogram

15–20 nm were obtained for CuO-NPs. The size distribution of the synthesized CuO-NPs was assessed using DLS analysis (Fig. 1 (d)). The obtained result indicated that the size of CuO-NPs was in the range of 3-200 nm. Moreover, the average diameter of synthesized CuO-NPs was estimated to be 43 nm. In conclusion, CuO-NPs were successfully synthesized with high purification.

Characterization of SPA

FTIR spectrum of the SPA is indicated in Fig. S1. There are several characteristic peaks at wavenumbers around 3411, 2917, 1759, 1640, 1388, 1068, and 523 cm^{-1} which are attributed to stretching vibration of hydroxyl groups (–OH), symmetric and asymmetric stretching of C-H, stretching of carbonyl (C = O), stretching of C = C, scissors of methylene (CH_2), stretching of C-O, and stretching of CH = CH [39], respectively. These results indicated that SPA possesses flavonoid and phenolic components. Moreover, according to these results, SPA was successfully extracted.

pH-sensitivity and UV-Vis absorption of SPA solution anthocyanins possess the potential to change color in specific conditions, such as different pH buffer solutions [40]. Color response and UV-Vis absorption spectra of SPA in various pH buffer solutions (2–12) are presented in Fig. 2 (a) and (b). SPA solution illustrated different color responses in various pH buffer solutions: red at pH 2–3, bright red at pH 4–5, pale pink at pH 6–7, green-blue at pH 8–9, bright green at pH 10, and bright yellow at pH 11–12. The observed color response is relevant to the transformation of

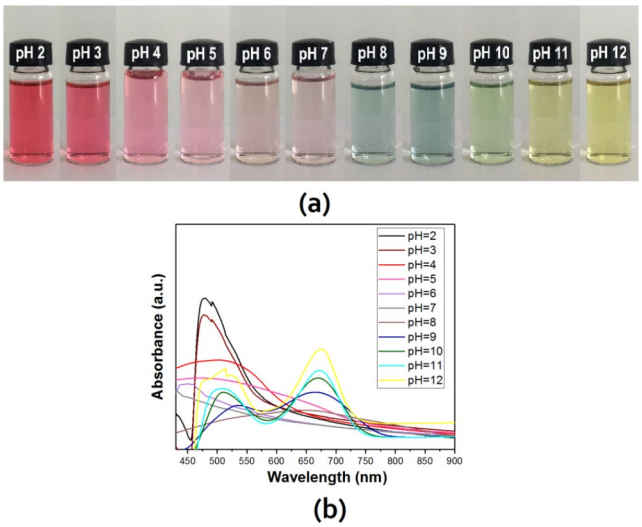

Fig. 2 SPA in various pH buffer solutions: (a) color variations, (b) UV-Vis spectra

the anthocyanin molecules, such as flavylium structure (pH 2–3) to chalcone structure (pH 11–12) [18]. It is well known that changing pH solution of anthocyanins can transfer the wavelength and intensity absorption of the peaks [41]. Figure 2 (b) demonstrates the UV-Vis absorption spectra of SPA in different pH solutions. The absorption wavelength of SPA in acidic solution (pH 2) sharply appeared at the center of 490 nm. Notably, when the pH value of SPA was increased from 2 to 7, the absorption intensity decreased. However, in alkaline media (by raising the pH from 8 to 12), the intensity of the absorption peak increased, and the position of wavelength transferred to the center of 670 nm. Similar observations have been reported by Zeng et al., (2019), who extracted mulberry anthocyanins from mulberry juice by solvent extraction method. They reported that the maximum absorption peak of mulberry anthocyanins appeared at the center of 512 nm in acidic solution (pH 2–3) and by increasing pH to 7, a red shift was observed and the intensity decreased. In the alkaline medium, by increasing the pH value, the intensity of the peak increased [42].

Characterization of bio-based films

Mechanical properties of bio-based films

The mechanical properties of the prepared bio-based films were determined, and the results were summarized in Table 1. Two mechanical parameters, including tensile strength and young's modulus slightly decreased by incorporating SPA (2% wt) into the bio-based CMCS film. However, the elongation at the break of this film increased. This effect can be due to the interaction of CMCS and SPA that can act as a plasticizer in bio-based films [22]. Plasticizers can increase the movement of the polymer chains, leading to an increase in the flexibility of the films. Similar results have been reported by Nogueira et al., (2018) who investigated the effect of blackberry powder on the physicochemical properties of arrowroot starch films. They found that the films containing blackberry powder represented more flexibility compared to neat film due to the plasticizing effect of blackberry powder [43]. The effect of different concentrations of CuO-NPs on the mechanical properties of the bio-based films was also evaluated and the results were reported in Table 1. By incorporating CuO-NPs into the films up to a certain point (1%), tensile strength increased significantly ($p<0.05$), but beyond that, tensile strength decreased. These results can be related to the quality of dispersion of nanoparticles into the polymer matrix. In other words, the high content of nanoparticles (1.5% wt) can lead to the creation of several aggregations in the polymer matrix. These aggregations can act as defect sites in the polymer matrix leading to faster failure [23]. However, the low content of nanoparticles (0.5 and 1% wt) can appropriately transfer the stress from the matrix to nanoparticles [44].

With increasing CuO-NPs concentration, the elongation at break showed a decreasing trend. This phenomenon can be assigned to the presence of nanoparticles in the polymer matrix leading to restriction of the polymer chains movement. The higher nanoparticles content incorporated in the polymer matrix, the higher restriction movement for the polymer chains is created [45].

UV-Vis absorption analysis of bio-based films

UV-Vis absorption spectra of the fabricated bio-based films, including neat CMCS, CMCS-SPA-2, and CMCS-SPA-2-CuO-1 are depicted in Fig. 3. In the case of neat CMCS, there is no absorption peak in the UV region; however, the broad absorption peak was appeared in the range of 220–320 nm for CMCS incorporated with SPA. This phenomenon can be related to the intrinsic ability of SPA to absorb the

Table 1 Textural properties of CMCS based films incorporated with SPA and CuO NPs*

Samples	Tensile Strength (MPa)	Elongation (%)	Young's Modulus (MPa)
CMCS	24.25 ± 1.1^{b}	19.74 ± 0.7^{b}	528.87 ± 12.5^{bc}
CMCS-SPA-2	22.08 ± 0.9^{bc}	21.35 ± 1.0^{a}	515.14 ± 10.2^{c}
CMCS-CuO-0.5	25.87 ± 1.8^{b}	16.42 ± 0.3^{d}	531.76 ± 14.6^{b}
CMCS-SPA-2-CuO-0.5	24.13 ± 1.3^{b}	18.13 ± 0.2^{c}	522.40 ± 12.8^{b}
CMCS-CuO-1	31.20 ± 2.0^{a}	14.93 ± 0.8^{e}	549.32 ± 16.5^{a}
CMCS-SPA-2-CuO-1	30.70 ± 1.7^{a}	15.44 ± 1.7^{e}	542.65 ± 11.3^{a}
CMCS-CuO-1.5	20.13 ± 1.0^{c}	9.84 ± 0.6^{f}	552.03 ± 18.9^{a}
CMCS-SPA-2-CuO-1.5	19.01 ± 1.2^{c}	10.67 ± 0.7^{f}	547.54 ± 17.0^{ab}

*a, b, c, d, e and f, different letters in the same column indicate significant differences at 5%

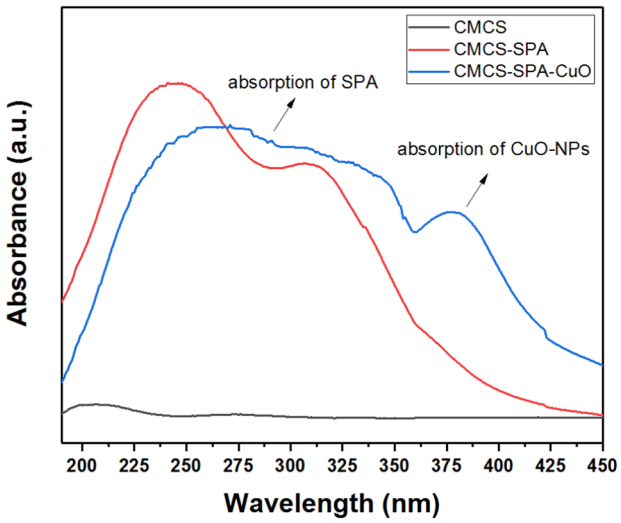

Fig. 3 UV-Vis absorption spectra of fabricated bio-based films, including CMCS, CMCS-SPA-2, and CMCS-SPA-2-CuO-1

UVC and UVB regions. The same result has been reported by Alizadeh-Sani et al. (2021), who showed that incorporating saffron petal anthocyanin into the methylcellulose/chitosan nanofiber films created a strong UV light barrier in $\lambda < 370$ nm due to the ability of anthocyanin to absorb the UV radiation. In the spectrum of CMCS-SPA-2-CuO-1 film, two broad and narrow absorption peaks were detected in the range of 230–326 nm (UVC-UV-B) and 340–380 nm (UVA), which are due to the absorption peak of SPA as anthocyanin agent and CuO-NPs (as semiconductor material (surface plasmon resonance (SPR)), respectively [46]. Interestingly, SPA and CuO-NPs in the CMCS film simultaneously cover the broad absorption in the UV region (UVA, UVB, and UVC). This specific property (UV shielding) of CMCS-SPA-2-CuO-1 film creates a chance as an excellent candidate to be used in food packaging applications.

Microstructure analysis of bio-based films

The cryo-fractured surface morphology and elemental analysis of the fabricated bio-based films were determined by FE-SEM and EDX analyses, respectively. Figure 4 demonstrates the micrographs of CMCS, CMCS-SPA-2, and CMCS-SPA-2-CuO-1 films. As shown in Fig. 4a, CMCS bio-based film showed a uniform and flat surface, which is attributed to the absence of any impurities and the proper preparation in the section of fracture under liquid nitrogen. In the case of CMCS-SPA-2 (Fig. 4b), no change was observed on the cryo-fractured surface of the bio-based film. This observation is due to the appropriate dispersion of SPA in the CMCS film. Notably, by adding CuO-NPs to the CMCS-SPA film, several white sphere-like spots were appeared (Fig. 4c), which can be due to the presence of CuO-NPs. To confirm this observation, the elemental analysis was conducted and the results revealed that CuO-NPs were dispersed into the bio-based film (Fig. 4f). This phenomenon can therefore lead to creating a rougher surface compared to neat CMCS and CMCS-SPA films.

Thermal stability analysis of bio-based films

Figure 5 shows the TGA curves of CMCS, CMCS-SPA-2, and CMCS-SPA-2-CuO-1 films. In the case of neat CMCS and CMCS-SPA-2 films, three stages weight loss was observed. The first-stage occurred in the range of 65–170 °C, which could be related to the evaporation of water molecules from the fabricated films [35]. The second stage happen at around 190–360 °C, which could be attributed to the evaporation of glycerol [15]. The third stage involved a significant weight loss in the range of 420–550 °C, which could be assigned to degradation of CMCS backbone and SPA [18]. In the specimen of CMCS-SPA-2-CuO-1 film, three stages decomposition in the range of 65–180 °C, 195–380 °C, and 450–530 °C were observed. The first and second stages were similar to other films (dehydration and evaporation of glycerol). The third stage could be associated with the degradation of CMCS backbone, SPA, and organic compounds from synthesizing CuO-NPs [47]. It should be noted that incorporation of SPA into the CMCS did not considerably change the thermal behavior of neat CMCS film. However, incorporating CuO-NPs into CMCS-SPA-2 film led to superior thermal stability compared to the neat CMCS and CMCS-SPA-2 films. It can be suggestively assigned to diminishing the mobility of the polymer chain and the limitation of the gas flow during the decomposition [48]. Similar results have been reported by Zhang et al., (2019) who investigated the effect of TiO_2 nanoparticles and/or black plum peel extract on the thermal stability of the chitosan films. They reported that incorporating TiO_2 nanoparticles

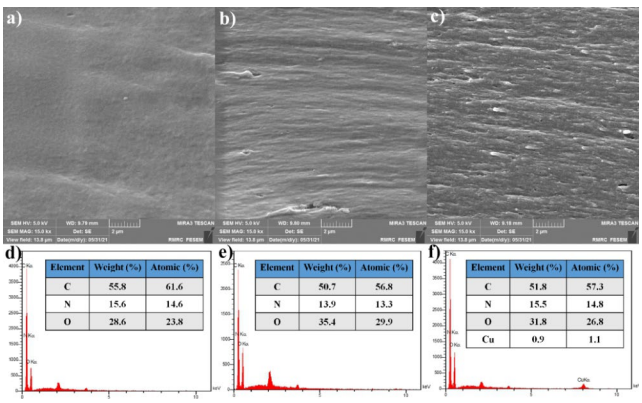

Fig. 4 Cryo-fractured surface morphology of (a) CMCS, (b) CMCS-SPA-2, (c) CMCS-SPA-2-CuO-1 bio-based films and EDX patterns of (d) CMCS, (e) CMCS-SPA-2, (f) CMCS-SPA-2-CuO-1 bio-based films

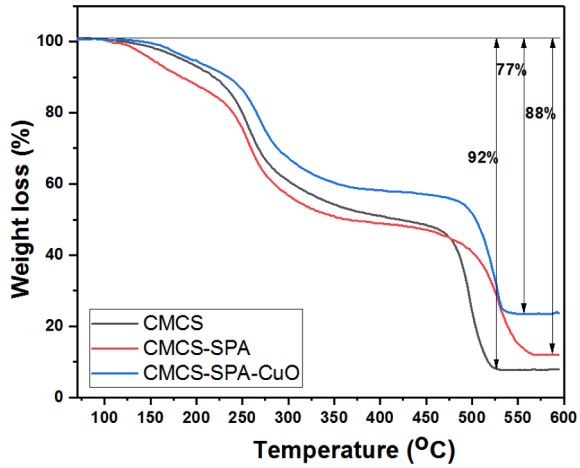

Fig. 5 TGA curve of CMCS, CMCS-SPA-2, and CMCS-SPA-2-CuO-1 films

improved the thermal stability of prepared films owing to the ability of TiO_2 nanoparticles to diminish the mobility of polymer chain and thermal resistance of the mentioned nanoparticles [48].

Physical properties of bio-based films

Physical properties of the prepared bio-based films, including MC, WS, and WCA are shown in Table 2 and Fig S2. It can be seen that the MC of the bio-based film did not significantly change by incorporating SPA into the CMCS film ($p<0.05$). However, the incorporation of CuO-NPs into the CMCS-SPA-2 film resulted in the reduction of the MC from 11.63 to 8.54%, which could be related to the surface morphology of the prepared bio-based films and interaction between CuO-NPs and CMCS-SPA-2 films. This interaction acts as a hindrance for the diffusion of the water molecules into the bio-based film [49].

Table 2 The moisture content, water solubility, and water contact angle results of the fabricated bio-based films

Samples	Moisture content (%)	Water solubility (%)	Water contact angle (°)
CMCS	11.63 ± 0.2^{a}	86.32 ± 1.2^{b}	78.6 ± 1.6^{b}
CMCS-SPA-2	10.97 ± 0.1^{b}	90.18 ± 1.0^{a}	66.3 ± 2.9^{c}
CMCS-SPA-2-CuO-1	8.54 ± 0.3^{c}	81.72 ± 0.9^{c}	95.1 ± 2.7^{a}

*a, b and c, different letters in the same column indicate significant differences at 5%

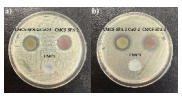

Fig. 6 Photos of antibacterial activity of the fabricated bio-based films in the disc diffusion method against (a) *S.aureus*, (b) *E.coli*

It was also observed that when SPA was added to the film formulation, WS of CMCS film increased; however, the WCA of this film decreased. These results is due to the hydrophilic nature of SPA. The same result has been reported by Mei et al., (2020) who evaluated the effect of different concentrations of torch ginger extract on the water solubility of sago starch. They found that the water solubility of the films increased by incorporating different concentrations of the extract which could be associated with its hydrophilic nature [21]. In the case of CMCS-SPA-2-CuO-1 film, the addition of CuO-NPs to the CMCS-SPA led to a reduction in WS and an increase of the WCA, which is attributed to the hydrophobic nature of CuO-NPs and interaction of CuO-NPs and CMCS matrix. In other words, by incorporating CuO-NPs into the bio-based film, the surface roughness of the films increased, resulting in diminishing the hydrophilicity [50]. In conclusion, CuO-NPs play an important role to diminish the WS of the CMCS-SPA film leading to the CMCS-SPA-2-CuO-1 film applicable in food packaging.

Antibacterial activity of bio-based films

Figure 6; Table 3 illustrate the antibacterial activity of the fabricated bio-based films including CMCS, CMCS-SPA-2 and CMCS-SPA-2-CuO-1 against *Staphylococcus aureus* (*S.aureus*) (PTCC 1112 (ATCC 6538p)) as Gram-positive and *Escherichia coli* (*E.coli*) (ATCC 25,922) as Gram-negative bacteria. The obtained results indicated that CMCS did not show any inhibition effect against two species of bacteria. While CMCS/ SPA films could inhibit the growth of two tested bacteria. By attention to Table 3, inhibition zones diameter of CMCS-SPA-2 film were ~ 10 and ~ 13 mm for *S.aureus* and *E.coli*, respectively. This effect is due to the presence of flavonoids in SPA composition [51]. Jafari-sales et al. (2020) reported that extracted saffron petal had antibacterial activity against two Gram-positive (*B.cereus* and *S.aureus*) and Gram-negative (*E.coli* and *P. aeruginosa*) bacteria [52]. The film containing SPA and CuO-NPs demonstrated a higher diameter of inhibition zone against both bacteria compared to CMCS-SPA-2 film. This enhancement can be attributed to the presence of CuO-NPs. It is well known that CuO-NPs can able to adhere to the cell membrane and generate reactive oxygen species. These reactions can prevent nutrition entry into the cell of bacteria and serious damage to the cell membrane, subsequently, inhibit the growth of bacteria [53]. The inhibition zone for *S.aureus* was greater when compared to *E.coli* which can be due to differences in the structure of bacteria. *S.aureus* as Gram-positive bacteria does not possess an outer membrane (lipid-based impermeable outer membrane) in the structure that antibacterial agents can destroy the bacteria by penetration into the cell simply. Overall, CMCS-SPA-2-CuO-1 bio-based film

Table 3 Zone inhibition diameter (mm) of bio-based films against both bacteria*

Samples	CMCS	CMCS-SPA-2	CMCS-SPA-2-CuO-1
E. coli	0	12.5 ± 0.2^{bB}	14.1 ± 0.1^{bA}
S. aureus	0	13.3 ± 0.4^{aB}	15.8 ± 0.3^{aA}

* Different small letters in the same column indicate significant differences between different strains of bacteria for same sample ($P < 0.05$). Different capital letters in the same row indicate significant difference between different films for same bacteria ($P < 0.05$)

could be used as an effective active packaging for extending the shelf life of food.

***In-vitro*toxicity of bio-based films**

Figure 7 represents HDF cell viability and attachment on the fabricated bio-based films. As shown in Fig. 7 (a), no notable difference was observed in cell viability of the neat CMCS, and the control group. In other words, there is no toxicity effect on the specimen of CMCS indicating acceptable bio-safety. This result could be attributed to the intrinsic biocompatibility of bio-polymers [54]. However, the cell viability of CMCS film significantly reduced by the incorporation of CuO-NPs ($p<0.05$). This means that CMCS-CuO-1 nanocomposite film represents a toxic effect that could be assigned to the release of Cu ions from the surface of the fabricated film. The same result has been reported by other researchers that the addition of semiconductor nanoparticles on the polymer matrix led to a toxic effect [35]. Interestingly, in the case of CMCS-SPA-2-CuO-1 film, the cell viability was higher than that of CMCS-CuO-1 film, which means that the mentioned film is bio-safe (higher than 80% cell viability). This observation could be related to the presence of SPA in the nanocomposite film, leading to the enhancement of the cell attachment by increasing the hydrophilicity of the fabricated film [55]. Moreover, SPA as an antioxidant agent can reduce the release of Cu ions (chelating effect), decreasing toxicity. Similar results have been reported by Sun et al., (2018). They extracted purple sweet potato anthocyanins (PSPAs) from Chinese purple sweet potato cultivar (Ipomoea batatas (L.) Lam.) and reported that PSPAs represented high potential to reduce Fe^{2+} by chelating effect [13]. Figure 7 (b) exhibits the attachment of the HDF cells to the prepared bio-based films by the 4', 6-diamidino-2-phenylindole (DAPI) staining technique. The mentioned technique shows the amount of cell adhesion on the surface of the prepared films by displaying the core of viable cells. As shown in Fig. 7 (b), in the case of CMCS-CuO-1 film, the number of living cells significantly diminished compared to the pure CMCS film, which indicates the poor cell attachment ability of the fabricated nanocomposite film. On the contrary, in the specimen of CMCS-SPA-2-CuO-1 film, the number of the living cell was higher compared to the CMCS-CuO-1 nanocomposite film. These results indicated that the presence of SPA in the bio-based film could facilitate the cell adhesion process on the surface of the bio-based film resulting in improving the bio-safety of the fabricated film.

Color response-ability of the bio-based pH indicator film

The optimized film (CMCS-SPA-2-CuO-1) was immersed in different pH buffer solutions and the response of the color change was presented in Fig. 8. CMCS-SPA-2-CuO-1 film exhibited a light brown color originating from the color of CuO-NPs. It can be seen that the color of the optimized film was dependent on the pH changes due to the presence of anthocyanin as a pH indicator [42]. The fabricated CMCS-SPA-2-CuO-1 film showed the pink and green color at the acidic (pH 3 and 5) and alkaline (pH 9 and 11) media, respectively, which could be related to transformation SPA structure [18]. In order to confirm this observation, color parameters were determined (Table 4). The values of a^* and b^* parameters changed in different pH buffer solutions. Moreover, the values of ΔE^* showed that the changes in the color of the fabricated films can be recognized by human eye [56]. The obtained result revealed that the color response of the optimized film was nearly similar to the obtained result from the color responses of SPA solution to pH changes (Sect. 3.2). In other words, the incorporation of CuO-NPs could not significantly affect the pH-sensitive ability of the

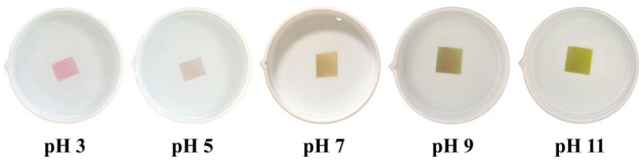

Fig. 8 Color change of CMCS-SPA-2-CuO-1 bio-based film to different pH buffer solutions

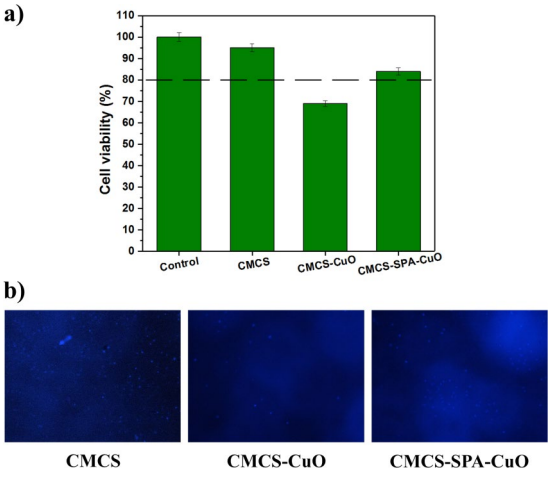

Fig. 7 The cell viability of HDF fibroblast cells cultured on the bio-based films, including CMCS, CMCS-CuO-1, and CMCS-SPA-2-CuO-1 (a), and fluorescent microscopy images of DAPI stained nuclei of the cells after 12 h of culture on the bio-based films (b)

Table 4 Color parameters (L*, a*, b* and ΔE*) of the bio-based film in different pH buffer solutions

Samples	L*	a*	b*	ΔE*
CMCS-SPA-2-CuO-1 (pH 7)	71.79 ± 4.5^{b}	4.11 ± 0.3^{c}	31.54 ± 4.2^{b}	38.11
CMCS-SPA-2-CuO-1 (pH 9)	63.38 ± 2.1^{d}	-1.16 ± 0.3^{d}	29.64 ± 2.3^{b}	41.69
CMCS-SPA-2-CuO-1 (pH 11)	68.31 ± 2.0^{c}	-10.19 ± 1.5^{e}	50.89 ± 3.6^{a}	57.32
CMCS-SPA-2-CuO-1 (pH 5)	81.80 ± 2.9^{a}	6.86 ± 0.8^{b}	7.18 ± 1.0^{c}	14.86
CMCS-SPA-2-CuO-1 (pH 3)	74.69 ± 3.4^{b}	17.16 ± 1.0^{a}	3.33 ± 0.5^{d}	25.25

*a, b, c and d, different letters in the same column indicate significant differences at 5%

optimized film. The same result has been reported by Zhang et al., who investigated the effect of TiO_2 nanoparticles and black plum peel extract on the physiochemical properties of chitosan films. They indicated that incorporating nanoparticles can slightly alter the pH-sensitive ability of the films [48]. Therefore, CMCS-SPA-2-CuO-1 film exhibited high potential to be applied as a pH-indicator film in acidic and alkaline conditions.

Application of bio-based film as freshness/spoilage indicator

Microorganisms and enzymes are the main reasons for spoilage of the meat products during storage [57]. They can lead to the formation of nitrogen-based volatile compounds and increase the pH value. The generation of these compounds is due to the decomposition of proteins [18]. Figure 9 shows the use of CMCS-SPA-2-CuO-1 bio-based film as an indicator to detect the freshness, onset of spoilage and completely spoilage of the lamb meat as a food model product. As shown in Table 5, when the samples were stored at 4 °C, with increase of storage time from 0 to 72 h, the pH value and TVB-N content increased from 5.87 to 6.79 and 8.32 to 19.52 (mg/100 g), respectively ($p<0.05$). Similarly, at 25 °C, with increasing time of storage from 0 to 12 h, the pH value and TVB-N content increased from 5.87 to 6.45 and 8.32 to 20.45 (mg/100 g), respectively ($p<0.05$). Based on these observations, the onset of spoilage in the tenderized meat was detected after 72 h of storage time at 4 ˚C and 12 h at 25 ˚C by attention to the TVB-N level (according to the literature, TVB-N value for fresh meat is ≤ 20 mg/100 g) [3, 37]. As shown in Fig. 9 and Table S1 in the supplemental material, the color of the optimized bio-based film clearly changed from light brown (fresh meat) to pastel grey (onset of spoilage) and then it became green (completely spoilage) during several days of storage at 4 and 25 °C. This change in the color can be due to the formation of volatile nitrogenous compounds and the increase in the pH value of the meat sample. In conclusion, the optimized film (CMCS-SPA-2-CuO-1) can be suitable candidate for monitoring the freshness/spoilage of lamb meat during storage.

Conclusions

In this study, two additive materials (SPA and CuO-NPs) were successfully prepared and were incorporated into the CMCS matrix to fabricate a new pH-indicator film. The mechanical result revealed that SPA can act as a plasticizer in CMCS films. UV-Vis absorption of CMCS-SPA-CuO film indicated the broad absorption peaks in the range of 230–320 nm (UVC-UVB) and 340–380 nm (UVA). Notably, incorporating CuO-NPs significantly increased the thermal stability, roughness, mechanical and antibacterial properties of the films; while reduced the moisture content and water solubility of the CMCS-SPA films. Finally, the optimized CMCS bio-based film containing 2% wt SPA and 1% wt CuO-NPs exhibited a bio-safe and pH-sensitive property against HDF cells and acidic/alkaline media, respectively.

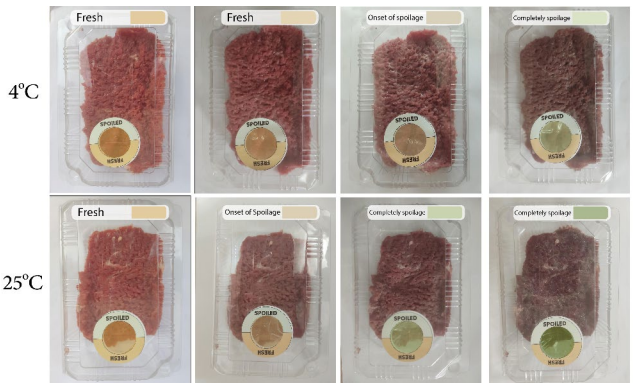

Fig. 9 Change in the color of CMCS-SPA-2-CuO-1 bio-based film as a pH indicator to monitor the freshness/spoilage of tenderized meat in 4 ˚C at 0, 48, 72, 120 h and 25 ˚C at 0, 12, 48, 72 h after attachment inside the polypropylene box

Table 5 the change of pH and TVB-N values in the lamb meat at different storage times

Time (h)	pH	TVB-N (mg/100 g)	Temperature (˚C)
0	5.87 ± 0.22^{e}	8.32 ± 1.1^{f}	25
12	6.45 ± 0.31^{cd}	20.45 ± 2.4^{d}	25
48	7.21 ± 0.19^{b}	47.16 ± 4.9^{b}	25
72	8.81 ± 0.23^{a}	80.31 ± 4.6^{a}	25
0	5.87 ± 0.09^{e}	8.32 ± 1.8^{f}	4
48	6.09 ± 0.12^{d}	14.89 ± 2.3^{e}	4
72	6.79 ± 0.10^{c}	19.52 ± 2.1^{d}	4
120	7.29 ± 0.19^{b}	29.46 ± 3.0^{c}	4

*a, b, c, d, e and f, different letters in the same column indicate significant differences at 5%

Therefore, multifunctional CMCS-SPA-2-CuO-1 film possesses the outstanding potential to give valuable information about the freshness/spoilage of the meat as a food product for fabrication of intelligent packaging applications.

Electronic supplementary material The online version of this article (doi:https://doi.org/10.1007/s10924-022-02490-6) contains supplementary material, which is available to authorized users.

Declaration of Interest Statement Authors declare that they are free of any conflicts of interest.

References

1. Sun J, Jiang H, Wu H, Tong C, Pang J, Wu C (2020) Multifunctional bionanocomposite films based on konjac glucomannan/chitosan with nano-ZnO and mulberry anthocyanin extract for active food packaging. Food Hydrocoll 107:105942
2. Perera KY, Jaiswal S, Jaiswal AK (2022) A review on nanomaterials and nanohybrids based bio-nanocomposites for food packaging. Food Chem 376:131912
3. Capello C, Trevisol TC, Pelicioli J, Terrazas MB, Monteiro AR, Valencia GA (2021) Preparation and characterization of colorimetric indicator films based on chitosan/polyvinyl alcohol and anthocyanins from agri-food wastes. J Polym Environ 29:1616–1629
4. Fathi M, Rostami H, Youseftabar Miri N, Samadi M, Delkhosh M (2022) Development of an intelligent packaging by incorporating curcumin into pistachio green hull pectin/poly vinyl alcohol (PVA) films. J Food Meas 16:1–10
5. Kabir E, Kaur R, Lee J, Kim K-H, Kwon EE (2020) Prospects of biopolymer technology as an alternative option for non-degradable plastics and sustainable management of plastic wastes. J Clean Prod 258:120536
6. Ding L, Li X, Hu L, Zhang Y, Jiang Y, Mao Z, Xu H, Wang B, Feng X, Sui X (2020) A naked-eye detection polyvinyl alcohol/cellulose-based pH sensor for intelligent packaging. Carbohydr Polym 233:115859
7. Liu Y, Zhang X, Li C, Qin Y, Xiao L, Liu J (2020) Comparison of the structural, physical and functional properties of κ-carrageenan films incorporated with pomegranate flesh and peel extracts. Int J Biol Macromol 147:1076–1088
8. Bai R, Zhang X, Yong H, Wang X, Liu Y, Liu J (2019) Development and characterization of antioxidant active packaging and intelligent Al3+-sensing films based on carboxymethyl chitosan and quercetin. Int J Biol Macromol 126:1074–1084
9. Zhu A, Yuan L, Liao T (2008) Suspension of Fe3O4 nanoparticles stabilized by chitosan and o-carboxymethylchitosan. Int J Pharm 350:361–368
10. Sun J, Jiang H, Li M, Lu Y, Du Y, Tong C, Pang J, Wu C (2020) Preparation and characterization of multifunctional konjac glucomannan/carboxymethyl chitosan biocomposite films incorporated with epigallocatechin gallate. Food Hydrocoll 105:105756
11. Abdin M, Salama MA, Gawad RMA, Fathi MA, Alnadari F (2021) Two-Steps of Gelation System Enhanced the Stability of Syzygium cumini Anthocyanins by Encapsulation with Sodium Alginate, Maltodextrin, Chitosan and Gum Arabic. J Polym Environ 29:3679–3692
12. Ferarsa S, Zhang W, Moulai-Mostefa N, Ding L, Jaffrin MY, Grimi N (2018) Recovery of anthocyanins and other phenolic compounds from purple eggplant peels and pulps using ultrasonic-assisted extraction. Food Bioprod Process 109:19–28
13. Sun H, Zhang P, Zhu Y, Lou Q, He S (2018) Antioxidant and prebiotic activity of five peonidin-based anthocyanins extracted from purple sweet potato (Ipomoea batatas (L.) Lam.). Sci Rep 8:1–12
14. Capello C, Leandro GC, Gagliardi TR, Valencia GA (2021) Intelligent Films from Chitosan and Biohybrids Based on Anthocyanins and Laponite®: Physicochemical Properties and Food Packaging Applications. J Polym Environ 29:3988–3999
15. Yong H, Wang X, Bai R, Miao Z, Zhang X, Liu J (2019) Development of antioxidant and intelligent pH-sensing packaging films by incorporating purple-fleshed sweet potato extract into chitosan matrix. Food Hydrocoll 90:216–224
16. Dainelli D, Gontard N, Spyropoulos D, Zondervan-van den Beuken E, Tobback P (2008) Active and intelligent food packaging: legal aspects and safety concerns. Trends Food Sci Technol 19:S103–S112
17. Zhang J, Zou X, Zhai X, Huang X, Jiang C, Holmes M (2019) Preparation of an intelligent pH film based on biodegradable polymers and roselle anthocyanins for monitoring pork freshness. Food Chem 272:306–312
18. Alizadeh-Sani M, Tavassoli M, McClements DJ, Hamishehkar H (2021) Multifunctional halochromic packaging materials: Saffron petal anthocyanin loaded-chitosan nanofiber/methyl cellulose matrices. Food Hydrocoll 111:106237
19. Gutiérrez TJ (2018) Active and Intelligent Films Made from Starchy Sources/Blackberry Pulp. J Polym Environ 26:2374–2391
20. Hosseini A, Razavi BM, Hosseinzadeh H (2018) Saffron (Crocus sativus) petal as a new pharmacological target: a review. Iran J Basic Med Sci 21:1091
21. Mei LX, Nafchi AM, Ghasemipour F, Easa AM, Jafarzadeh S, Al-Hassan A (2020) Characterization of pH sensitive sago starch films enriched with anthocyanin-rich torch ginger extract. Int J Biol Macromol 164:4603–4612
22. Ezati P, Rhim J-W (2020) pH-responsive chitosan-based film incorporated with alizarin for intelligent packaging applications. Food Hydrocoll 102:105629
23. Zabihi E, Majidi HJ, Pasarvi SK, Shahrampour D, Goudarzi A, Khomeiri M, Hajiabdolrasouli M, Babaei A (2018) Fabrication and characterization of polyethylene nanocomposite films containing zinc oxide (ZnO) nanoparticles synthesized by a cost-effective and safe method. J Macromol Sci Part B: Phys 57:645–659
24. Tajdari A, Babaei A, Goudarzi A, Partovi R, Rostami A (2021) Hybridization as an efficient strategy for enhancing the performance of polymer nanocomposites. Polym Compos 42:6801–6815
25. Joz Majidi H, Babaei A, Kazemi-Pasarvi S, Arab-Bafrani Z, Amiri M (2021) Tuning polylactic acid scaffolds for tissue engineering purposes by incorporating graphene oxide-chitosan nanohybrids. Polym Adv Technol 32:1654–1666
26. Jabraili A, Pirsa S, Pirouzifard MK, Amiri S (2021) Biodegradable Nanocomposite Film Based on Gluten/Silica/Calcium Chloride: Physicochemical Properties and Bioactive Compounds Extraction Capacity. J Polym Environ 29:2557–2571
27. Abdolmohammadi S, Siyamak S, Ibrahim NA, Yunus WMZW, Rahman MZA, Azizi S, Fatehi A (2012) Enhancement of mechanical and thermal properties of polycaprolactone/chitosan blend by calcium carbonate nanoparticles. Int J Mol Sci 13:4508–4522
28. de Matos Fonseca J, Valencia GA, Soares LS, Dotto MER, Campos CEM, Moreira RdFPM, Fritz ARM (2020) Hydroxypropyl methylcellulose-TiO2 and gelatin-TiO2 nanocomposite films: Physicochemical and structural properties. Int J Biol Macromol 151:944–956
29. Grigore ME, Biscu ER, Holban AM, Gestal MC, Grumezescu AM (2016) Methods of Synthesis, Properties and Biomedical Applications of CuO Nanoparticles. Pharmaceuticals 9:75

30. Alswat AA, Ahmad MB, Hussein MZ, Ibrahim NA, Saleh TA (2017) Copper oxide nanoparticles-loaded zeolite and its characteristics and antibacterial activities. J Mater Sci Technol 33:889–896
31. Aziz N, Mat Nor N, Arof A (2020) Optimization of anthocyanin extraction parameters from M. malabathricum via response surface methodology to produce natural sensitizer for dye sensitized solar cells. Opt Quantum Electron 52:1–13
32. Negahdari M, Partovi R, Talebi F, Babaei A, Abdulkhani A (2021) Preparation, characterization, and preservation performance of active polylactic acid film containing Origanum majorana essential oil and zinc oxide nanoparticles for ground meat packaging. J Food Process Preserv 45:e15013
33. Salarbashi D, Tafaghodi M, Bazzaz BSF, Mohammad Aboutorabzade S, Fathi M (2021) pH-sensitive soluble soybean polysaccharide/SiO2 incorporated with curcumin for intelligent packaging applications. Food Sci Nutr 9:2169–2179
34. Rukmanikrishnan B, Ramalingam S, Lee J (2021) Quaternary ammonium silane-reinforced agar/polyacrylamide composites for packaging applications. Int J Biol Macromol 182:1301–1309
35. Kazemi-Pasarvi S, Golshan Ebrahimi N, Shahrampour D, Arab-Bafrani Z (2020) Reducing cytotoxicity of poly (lactic acid)-based/zinc oxide nanocomposites while boosting their antibacterial activities by thymol for biomedical applications. Int J Biol Macromol 164:4556–4565
36. Seyedabadi MM, Rostami H, Jafari SM, Fathi M (2021) Development and characterization of chitosan-coated nanoliposomes for encapsulation of caffeine. Food Biosci 40:100857
37. Kuswandi B, Nurfawaidi A (2017) On-package dual sensors label based on pH indicators for real-time monitoring of beef freshness. Food Control 82:91–100
38. Reyes-Torres MA, Mendoza-Mendoza E, Miranda-Hernández ÁM, Pérez-Díaz MA, López-Carrizales M, Peralta-Rodríguez RD, Sánchez-Sánchez R, Martinez-Gutierrez F (2019) Synthesis of CuO and ZnO nanoparticles by a novel green route: Antimicrobial activity, cytotoxic effects and their synergism with ampicillin. Ceram Int 45:24461–24468
39. Mortazavi SM, Kamali Moghaddam M, Safi S, Salehi R (2012) Saffron Petals, a by-product for dyeing of wool fibers⁉ Prog Color Color Coat 5:75–84
40. Rodriguez-Amaya DB (2019) Update on natural food pigments - A mini-review on carotenoids, anthocyanins, and betalains. Food Res Int 124:200–205
41. Tang B, He Y, Liu J, Zhang J, Li J, Zhou J, Ye Y, Wang J, Wang X (2019) Kinetic investigation into pH-dependent color of anthocyanin and its sensing performance. Dyes Pigm 170:107643
42. Zeng P, Chen X, Qin Y-R, Zhang Y-H, Wang X-P, Wang J-Y, Ning Z-X, Ruan Q-J, Zhang Y-S (2019) Preparation and characterization of a novel colorimetric indicator film based on gelatin/polyvinyl alcohol incorporating mulberry anthocyanin extracts for monitoring fish freshness. Food Res Int 126:108604
43. Nogueira GF, Fakhouri FM, de Oliveira RA (2019) Effect of incorporation of blackberry particles on the physicochemical properties of edible films of arrowroot starch. Dry Technol 37:448–457
44. Liu L, Li L, Gao Y, Tang L, Zhang Z (2013) Single carbon fiber fracture embedded in an epoxy matrix modified by nanoparticles. Compos Sci Technol 77:101–109
45. Tajdari A, Babaei A, Goudarzi A, Partovi R (2020) Preparation and study on the optical, mechanical, and antibacterial properties of polylactic acid/ZnO/TiO2 shared nanocomposites. J Plast Film Sheeting 36:285–311
46. Apriandanu DOB, Yulizar Y (2019) Tinospora crispa leaves extract for the simple preparation method of CuO nanoparticles and its characterization. Nano-Struct Nano-Objects 20:100401
47. Nasrollahzadeh M, Sajadi SM, Rostami-Vartooni A, Hussin SM (2016) Green synthesis of CuO nanoparticles using aqueous extract of Thymus vulgaris L. leaves and their catalytic performance for N-arylation of indoles and amines. J Colloid Interface Sci 466:113–119
48. Zhang X, Liu Y, Yong H, Qin Y, Liu J, Liu J (2019) Development of multifunctional food packaging films based on chitosan, TiO2 nanoparticles and anthocyanin-rich black plum peel extract. Food Hydrocoll 94:80–92
49. Fonseca JdM, Valencia GA, Soares LS, Dotto MER, Campos CEM, Moreira RdFPM, Fritz ARM (2020) Hydroxypropyl methylcellulose-TiO2 and gelatin-TiO2 nanocomposite films: Physicochemical and structural properties. Int J Biol Macromol 151:944–956
50. Peighambardoust SJ, Peighambardoust SH, Pournasir N, Mohammadzadeh Pakdel P (2019) Properties of active starch-based films incorporating a combination of Ag, ZnO and CuO nanoparticles for potential use in food packaging applications. Food Packag Shelf Life 22:100420
51. Ghaheh FS, Mortazavi SM, Alihosseini F, Fassihi A, Nateri AS, Abedi D (2014) Assessment of antibacterial activity of wool fabrics dyed with natural dyes. J Clean Prod 72:139–145
52. Jafari-sales A, Pashazadeh M (2020) Antibacterial Effect of Methanolic Extract of Saffron Petal (Crocus sativus L.) on Some Standard Gram Positive and Gram Negative Pathogenic Bacteria In vitro. CUPMAP 3:1–7
53. Nouri A, Yaraki MT, Ghorbanpour M, Agarwal S, Gupta VK (2018) Enhanced Antibacterial effect of chitosan film using Montmorillonite/CuO nanocomposite. Int J Biol Macromol 109:1219–1231
54. Shariatinia Z (2018) Carboxymethyl chitosan: Properties and biomedical applications. Int J Biol Macromol 120:1406–1419
55. Eze FN, Jayeoye TJ, Singh S (2022) Fabrication of intelligent pH-sensing films with antioxidant potential for monitoring shrimp freshness via the fortification of chitosan matrix with broken Riceberry phenolic extract. Food Chem 366:130574
56. Merz B, Capello C, Leandro GC, Moritz DE, Monteiro AR, Valencia GA (2020) A novel colorimetric indicator film based on chitosan, polyvinyl alcohol and anthocyanins from jambolan (Syzygium cumini) fruit for monitoring shrimp freshness. Int J Biol Macromol 153:625–632
57. Wickramasinghe NN, Ravensdale J, Coorey R, Chandry SP, Dykes GA (2019) The predominance of psychrotrophic pseudomonads on aerobically stored chilled red meat. Compr Rev Food Sci Food Saf 18:1622–1635